Negative refraction of phonons and acoustic lensing effect of a crystalline slab

K. Imamura and S. Tamura
Department of Applied Physics, Hokkaido University, Sapporo 060-8628, Japan
(Received 10 May 2004; revised manuscript received 19 August 2004; published 30 November 2004)

We study how good a flat slab of a bulk crystalline solid with a large elastic anisotropy exhibits a lensing action for phonons or sound waves. The slowness and group-velocity surfaces of an ideal elastic solid for a flat phonon lens are analyzed in the geometrical acoustic approximation. These surfaces are compared with the corresponding surfaces of an existing bulk crystal (a zinc crystal) with hexagonal symmetry. To demonstrate the lensing effect we calculate the intensity distribution of phonons emitted from a point source in an isotropic medium (on one side of the lens), propagating through the slab lens and then transmitted into the isotropic medium in the other side. A similar calculation for sound waves with a finite-difference-time-domain method is performed to see the effects neglected in the geometrical acoustic approximation, that is, the effects of finite wavelength, mode conversion, and finite transmission at the interfaces.

DOI: 10.1103/PhysRevB.70.174308 PACS number(s): 63.20.−e, 62.65.+k, 66.70.+f, 68.65.Ac

I. INTRODUCTION

Recently, an electromagnetic (EM) wave propagation through an interface between a positive and negative refractive index material has attracted much attention.[1–8] An interesting observation is the fact that the refraction of the EM wave happens at the "wrong" side relative to the normal of the interface (a "negative refraction"). This provides a potential of fabricating a "superlens" which overcomes the diffraction limit of conventional lenses.[2] The material with a negative index of refraction (NIR) is sometimes called a left-handed material and can be realized, for example, with a specially designed photonic band gap material.[4,6–8] The negative refraction phenomena in photonic crystals happen in frequency regimes of negative group velocity either above the first frequency band (photonic band) near the Brillouin zone center or on the lowest photonic band near the Brillouin-zone corner farthest from the Γ point.[4,8]

A similar effect is expected to occur also for phonons or ultrasounds in phononic crystals, for instance.[9,10] Thus, we consider the analogous problem for phonons but in a system consisting simply of a bulk solid instead of an artificially designed material such as a phononic crystal. The presence of large elastic anisotropy and the resulting noncollinearity of the wave and group-velocity vectors in a crystalline solid[11–13] makes it possible that a bulk solid behaves as a material with a NIR. Accordingly, a parallel-sided slab of a crystal may exhibit a superlensing effect for a specific branch of phonons, i.e., the slow transverse (ST) phonons.[11] A desirable feature of a bulk crystal rather than the case of a phononic crystal is the fact that the negative refraction, if any, works for phonons (also sound waves) irrespective of frequencies as far as the lattice dispersion is neglected, i.e., up to several hundred GHz. It should be noted that in a phononic crystal (also in a photonic crystal) the lensing effect is highly frequency dependent.

Another merit is the focusing of phonons in the three dimensional space. The majority of the simulations made for the negative refraction and lensing effect of EM waves with photonic crystals are valid in two dimensions. With the structural anisotropy of the photonic crystals it is not clear if the photons or EM waves are really focused in the three dimensional space. In contrast, with a crystal of hexagonal symmetry exhibiting a transverse isotropy,[14,15] the focusing of phonons in three dimensions is guaranteed if the focusing in two dimensions is confirmed.

The organization of the present paper is as follows. In Sec. II, first we determine, with analytical calculations based on the geometrical acoustic approximation, the shapes of the slowness and group-velocity surfaces of phonons in an ideal elastic medium working as a flat phonon lens. Next, in Sec. III, we illustrate in the same approximation how a crystalline slab of zinc with hexagonal symmetry acts as a phonon lens. Finally, in order to take account of the effects neglected in the previous analyses, such as the effects of finite wavelength, mode conversion, and finite transmission at the interfaces, we develop a finite-difference-time-domain (FDTD) calculation[16–20] in Sec. IV and demonstrate how the sound waves excited at a point source propagate and produce a "point image" on the other side of the flat slab of zinc. In Sec. V we discuss the implication of the results we have obtained in the present work.

II. IDEAL MATERIAL FOR A FLAT PHONON LENS

First we analyze the conditions for the slowness and group-velocity surfaces of phonons in an ideal elastic solid working as a phonon lens. This analysis is made with the geometrical acoustic approximation. Let us consider the negative refraction effect of phonons in the system shown in Fig. 1, that is, a parallel-sided slab (the region II) of a transversally isotropic medium (similar to a hexagonal crystal with the c axis normal to the sides of the slab) is sandwiched in between two (identical) isotropic elastic solids (the regions I and III). Phonons are emitted from a point source O in the region I at a distance a apart from the edge of the region II. Those phonons are supposed to be focused at a point F in the region III (the distance h above the edge of the region II) after propagating through the anisotropic elastic slab, or phonon lens of thickness d.

Now we look for a desirable shape of the constant-frequency ($\omega=\omega_0$) surface or slowness surface in the wave

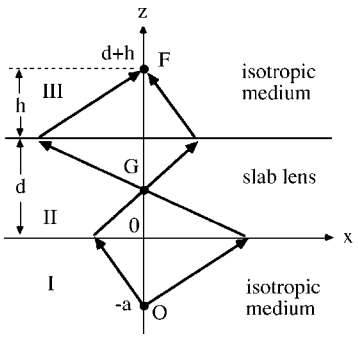

FIG. 1. A schematic of the geometry consisting of an ideal flat phonon lens of thickness d (the region labeled II) sandwiched in between the same isotropic elastic media (the regions labeled I and III). Phonon are launched from the point O at a distance a below the lower edge of the lens and focus at a focal point F above a distance h from the top of the lens. Phonons are also focused at a point G inside the lens.

vector $[\mathbf{k}=(k_x,k_y,k_z)]$ space of the lens material. Note that we assume a transverse isotropy for the lens and hence we may determine the section of the surface $k_z=f(k_x)$. The geometry for this assumed system (Fig. 1) leads to the differential equation

$$\frac{\left[\left(\frac{\omega_0}{c}\right)^2-k_x^2\right]^{1/2}}{k_x}\times\frac{df(k_x)}{dk_x}=\frac{a+h}{d}\equiv\beta, \tag{1}$$

where c is the sound velocity in the isotropic media I and III and β is the acoustic path length (along the z axis) in the isotropic media relative to that in the slab lens. This equation is readily solved to give

$$k_z=f(k_x)=-\beta\left[\left(\frac{\omega_0}{c}\right)^2-k_x^2\right]^{1/2}+\tilde{\gamma}, \tag{2}$$

where $\tilde{\gamma}=\tilde{\gamma}(\omega_0)$ is an integration constant independent of k_x. We see that the consistency with the linear elasticity theory requires that $\tilde{\gamma}(\omega_0)=\gamma\omega_0/c$ with γ a dimensionless constant related to the traveling time of phonons (see below). Equation (2) is equivalent to

$$k_x^2+\left(\frac{k_z-\gamma\frac{\omega_0}{c}}{\beta}\right)^2=\left(\frac{\omega_0}{c}\right)^2. \tag{3}$$

Thus the shape of the slowness curve in the lens material is an ellipse (the slowness surface is an ellipsoid).

Next we have to check if the phonons leaving from the point source O arrive at the focal point F at the same time irrespective of their traveling paths. We see that this is indeed the case and the traveling time is given by $t_0=\gamma d/c$. However, for those phonons focusing at the point F, there exists a restriction for their transverse component k_x of the initial wave vector. This is expressed as $|k_x|\leqslant\tilde{k}_c$, where

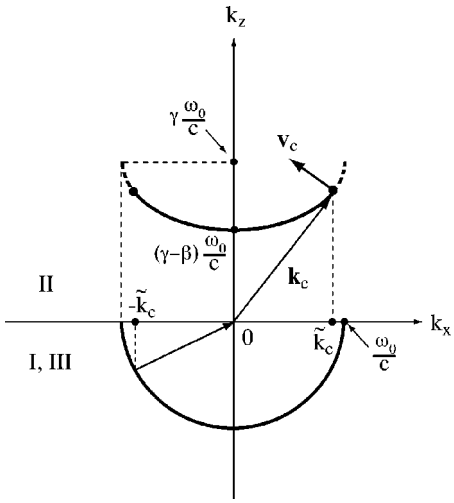

FIG. 2. Sections in the k_x-k_z plane of the constant-frequency $[\omega(\mathbf{k})=\omega_0]$ surfaces equivalent to the slowness surfaces of phonons in the isotropic media (the regions I and III with phonon phase velocity c) and in the ideal lens (the region II). $\mathbf{k}_c$ with the component $\tilde{k}_c$ along k_x axis is a critical wave vector in the ideal lens (satisfying $\mathbf{k}_c\perp\mathbf{v}_c$ with $\mathbf{v}_c$ a critical group velocity) for which the phonon has to travel with the infinite group velocity ($|\mathbf{v}_c|=\infty$) inside the lens.

$$\tilde{k}_c=\varepsilon\frac{\omega_0}{c}, \tag{4}$$

with $\varepsilon^2=1-\delta^2$ and $\delta\equiv\beta/\gamma=(a+h)/ct_0<1$. For $|k_x|=\tilde{k}_c$ phonons have to travel inside an ideal lens with an infinite speed, though this cannot happen in a real material. This situation is seen more clearly by calculating the group velocity $\mathbf{v}=\partial\omega/\partial\mathbf{k}$ of phonons. We find from Eq. (2)

$$v_x=\frac{-\beta ck_x}{\gamma\left[\left(\frac{\omega_0}{c}\right)^2-k_x^2\right]^{1/2}-\beta\frac{\omega_0}{c}}, \tag{5}$$

$$v_z=\frac{c\left[\left(\frac{\omega_0}{c}\right)^2-k_x^2\right]^{1/2}}{\gamma\left[\left(\frac{\omega_0}{c}\right)^2-k_x^2\right]^{1/2}-\beta\frac{\omega_0}{c}}. \tag{6}$$

From these equations we find $\mathbf{k}\cdot\mathbf{v}=\omega_0$. This is an important relation to be satisfied by $\mathbf{v}$ if the group-velocity is derived from the wave equation in the elasticity theory. For $k_x=\tilde{k}_c$ (or $k_x=-\tilde{k}_c$) the wave vector $\mathbf{k}=\mathbf{k}_c$ of the phonon in the lens is tangential to the slowness curve, hence perpendicular to the group velocity vector $\mathbf{v}=\mathbf{v}_c$. Accordingly, the above restriction leads to the infinite magnitude of $v_c=|\mathbf{v}_c|$, which can be also seen from the geometry of Fig. 2.

Now we see from Eqs. (5) and (6) the group-velocity curve is a hyperbola which is expressed as

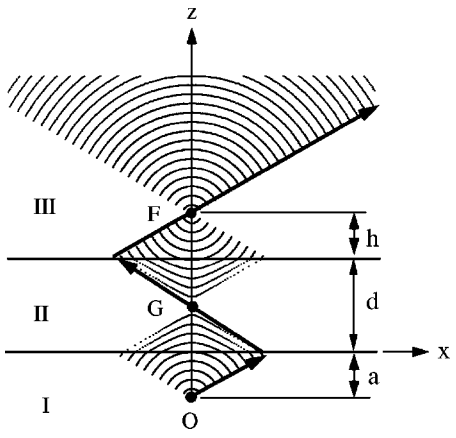

FIG. 3. Wave fronts in the ideal lens system calculated in the geometrical acoustic approximation with $\beta=1$ and $\gamma=2$. Arrows show a critical trajectory for which phonons have to travel with an infinite velocity inside the lens (the region II).

$$-\frac{v_x^2}{(\varepsilon c)^2}+\left(\frac{\gamma}{c}\right)^2\left(v_z-\frac{c}{\gamma\varepsilon^2}\right)^2=\left(\frac{\delta}{\varepsilon^2}\right)^2. \tag{7}$$

Incidentally, we note that phonons are also focused inside the lens at $x=0$ and $z=a/\beta=ad/(a+h)$ (point G), and at a time $\tilde{t}=a/\delta c$.

The shapes of the wave fronts in the geometrical acoustic approximation are displayed in Fig. 3 for $\beta=1$ and $\gamma=2$ ($a=h=d/2$). In the regions I and III they are circles expressed at a given time t as

$$x^2+(z+a)^2=(ct)^2, \quad \text{region I}, \tag{8}$$

$$x^2+(z-d-l)^2=c^2(t-t_0)^2, \quad \text{region III}, \tag{9}$$

and in the region II they are hyperbola described by

$$-\left(\frac{x}{\varepsilon}\right)^2+\gamma^2\left(z-\frac{ct-\delta a}{\gamma\varepsilon^2}\right)^2=\left(\frac{a-\delta ct}{\varepsilon^2}\right)^2. \tag{10}$$

A critical trajectory along which the phonons have to travel with an infinite group velocity inside the lens is shown by arrows. The phonons incident on the slab lens at an angle larger than this trajectory are reflected back from the interface and they are not shown in the plot of Fig. 3.

We also exhibit the calculated snapshot of the instantaneous density (or intensity) distribution of phonons in a stationary state in Fig. 4. Phonons are assumed to be emitted continuously from the point source O with a given time interval $\Delta t=1\times10^{-3}\,d/c$ with $a=d/4$. The initial propagation directions of phonons are uniform with an angular interval $\Delta\theta_{\mathbf{k}}=0.18°$. Also, we have subdivided the x-z plane into small grids with side lengths $\Delta x=\Delta z=5\times10^{-3}\,d$ and counted the number of phonons in each grid to obtain a phonon density distribution. Thus the darkness in Fig. 4(a) represents the relative densities of phonons and we find that they are focused at the focal point F ($h=0.672d$, so $\beta=0.922$ and $\gamma=5.92$)[21] as well as the point G inside the lens.

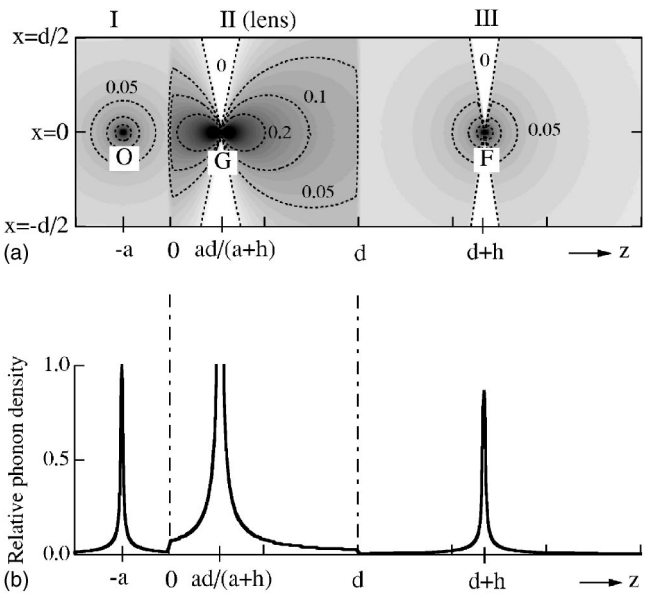

FIG. 4. (a) A snapshot of phonon density distribution in the x-z plane of an ideal lens system. (b) The relative phonon density along $x=0$ of (a). The density at the phonon source ($z=-a$) is normalized to unity. Several contours at low phonon density are shown in (a) by dashed lines. In these figures $a=0.25d$ and $h=0.67d$.

Here we note that in the medium with a slower phonon group velocity, the distance between the phonons emitted in a consecutive time interval becomes small, giving a larger phonon density distribution. This induces the phonon density distribution apparently discontinuous at interfaces, which is seen in Fig. 4 (and also Fig. 6 below) calculated based on the geometrical acoustic approximation. However, as shown in Fig. 7 (in Sec. IV), there exists no real discontinuity in the field intensity at the interfaces because the lattice displacement should be always continuous. The abrupt changes in phonon density at the interfaces are also understood by the fact that the wave field is large in an elastic medium with a small acoustic impedance but it is small in an elastic medium with large acoustic impedance when we consider the elastic wave propagation through an interface between the media with an impedance mismatch. In the present example, diamond has an acoustic impedance much larger than zinc and hence the lattice displacement and the associated phonon density is larger in zinc side of both interfaces.

Finally, it should be noted here that in Fig. 4 only a single mode of phonons is considered and neither the effect of transmission probability nor the effect of mode conversion at the boundaries between regions I and II and II and III are taken into account.

III. THE CASE OF HEXAGONAL CRYSTAL

Next we study how bulk crystalline solids resemble an ideal lens analyzed in the preceding section. This can be done first by relating the parameters β and γ of the ideal material to the mass density and elastic constants of an existing crystal. For this purpose we consider a hexagonal crystal which has the rotationally symmetry about the z axis, a

favorable property to focus phonons in three-dimensional space. Among three acoustic branches of phonons, only those of the ST branch exhibit negative refraction effect if the elastic constants satisfy an appropriate inequality. To see this we note that the slowness curve of the ST phonons is determined by

$$k_z^2 = \frac{1}{2c_{33}c_{44}}[(c_{33}+c_{44})\rho\omega^2 - (c_{11}c_{33}+c_{44}^2-\tilde{c}_{13}^2)k_x^2 + D^{1/2}], \tag{11}$$

where c_{IJ} is the Voigt elastic constants with two indices, $\tilde{c}_{13} \equiv c_{13}+c_{44}$ and

$$D = [(c_{11}c_{33}+c_{44}^2-\tilde{c}_{13}^2) - (c_{33}+c_{44})\rho\omega^2]^2 k_x^2 - 4c_{33}c_{44}[c_{11}c_{44}k_x^4 - (c_{11}+c_{44})k_x^2\rho\omega^2 + (\rho\omega^2)^2]. \tag{12}$$

Also the group-velocity of ST phonons in the x-z plane of a hexagonal crystal is

$$v_x = \frac{(c_{11}+c_{44})\rho\omega^2 - 2c_{11}c_{44}k_x^2 - (c_{11}c_{33}+c_{44}^2-\tilde{c}_{13}^2)k_z^2}{2\rho\omega^2 - (c_{11}+c_{44})k_x^2 - (c_{11}-c_{33})k_z^2} \times \frac{k_x}{\rho\omega}, \tag{13}$$

$$v_z = \frac{(c_{33}+c_{44})\rho\omega^2 - (c_{11}c_{33}+c_{44}^2-\tilde{c}_{13}^2)k_x^2 - 2c_{33}c_{44}k_z^2}{2\rho\omega^2 - (c_{11}+c_{44})k_x^2 - (c_{11}-c_{33})k_z^2} \times \frac{k_z}{\rho\omega}. \tag{14}$$

For a hexagonal crystal the ratio R of the elastic constants defined by

$$R = \frac{\tilde{c}_{13}^2}{c_{11}(c_{33}-c_{44})} \tag{15}$$

is an important parameter related to the shape of the slowness surfaces. For $R>1$ the slowness surface of the ST branch is concave along the k_z direction and exhibits the negative refraction for phonons.[14,15] This inequality is satisfied, for example, by zinc ($R=2.09>1$).[22]

Comparing the terms up to $O(k_x^2)$ in Eq. (11) with Eq. (2), the parameters β and γ are expressed in terms of the mass density and elastic constants of the hexagonal crystal. Thus we find

$$\beta = \frac{-c_l^2}{c_t c}(1-R), \tag{16}$$

$$\gamma = \frac{c}{c_t}\left[1 - \frac{c_l^2}{c^2}(1-R)\right], \tag{17}$$

where $c_{11}=\rho c_l^2$ and $c_{44}=\rho c_t^2$.

As far as we know, zinc is the best hexagonal crystal that has a large elastic anisotropy suitable for a lens material. In order that the phonons impinging on the slab lens are subjected to negative refraction irrespective of their wave vector directions, an elastically hard material with a small size of the slowness surface is required for a substrate of the lens. Hence, to demonstrate the lensing effect of zinc and compare with the case of ideal lens, we assume diamond (with isotropic approximation) as the isotropic media in the regions I and III, and thus c is the transverse sound velocity in diamond.

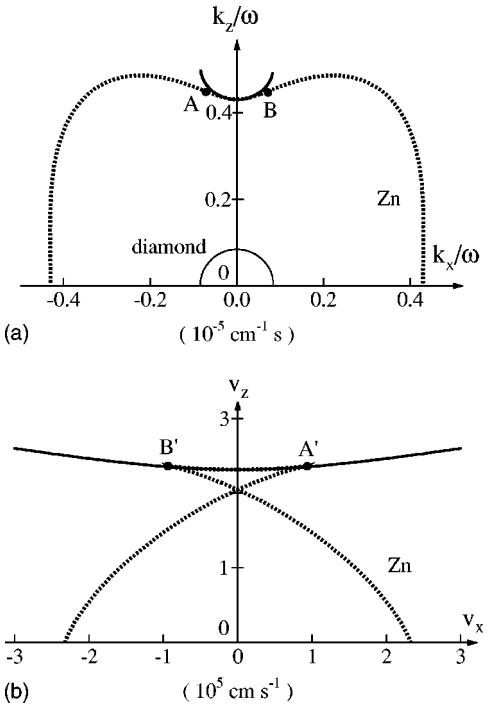

FIG. 5. Comparison of both the slowness and group-velocity curves of phonons in the ideal lens material (bold solid lines) and those of the slow-transverse phonons in zinc (dotted lines). (a) Sections of the slowness surfaces in the upper half of the k_x-k_z plane (the slowness curve of the transverse phonons in diamond is also illustrated by a thin solid line). (b) Sections of the group-velocity surfaces in the upper half of the v_x-v_z plane. The points labeled A and B in (a) are the inflection points of the slowness curve in Zn, which correspond to the folds A' and B' of the group-velocity curve in (b).

The slowness and group-velocity curves of ST phonons in zinc are compared in Fig. 5 with those of the ideal material with β and γ calculated from Eqs. (16) and (17).[23] The slowness curve in zinc well coincides with that of the ideal material only over the concave region in between A and B around the z axis. (The points A and B are the inflection points of the slowness curve but in the three-dimensional space they are the parabolic points with zero Gaussian curvature.) Although the size of this concave region on zinc is rather small, the negative refraction happens quite effectively when the phonons radiated from a diamond substrate are incident on a slab of zinc. We see in Fig. 5(b) that the group-velocity curve of ST phonons in zinc coincides very well with that in the ideal material in between the folds A' and B' defining caustic directions. These points A' and B' correspond to the inflection points A and B in the slowness curve.

For the diamond-Zn-diamond system assumed, the simulated snapshot of the instantaneous density distribution of the transverse mode (the ST mode inside the lens) has been illustrated in Fig. 6(a). The calculation has been carried out with the same condition as for Fig. 4. The focusing of

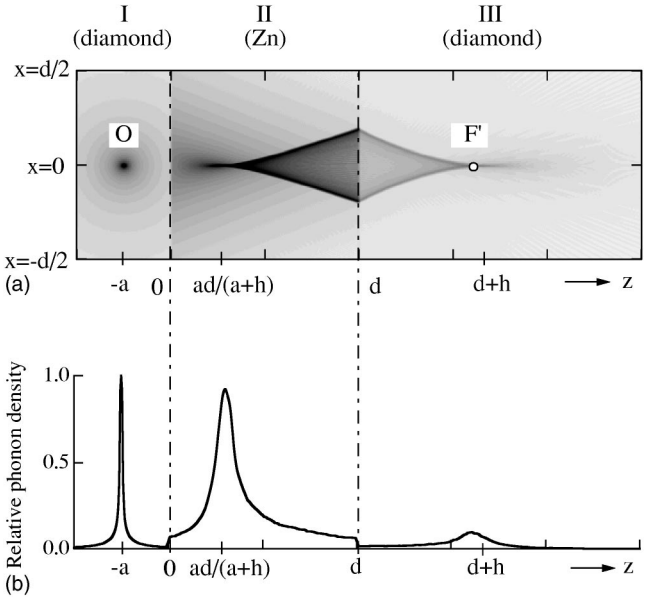

FIG. 6. (a) A snapshot of the density distribution of transverse phonons (slow-transverse phonons in zinc) in the x-z plane of a diamond-Zn-diamond system calculated in the geometrical acoustic approximation. (b) The relative phonon density along $x=0$ of (a). The density at the phonon source $z=-a$ is normalized to unity. In these figures $a=0.25d$ and $h=0.67d$ for the comparison with Fig. 4.

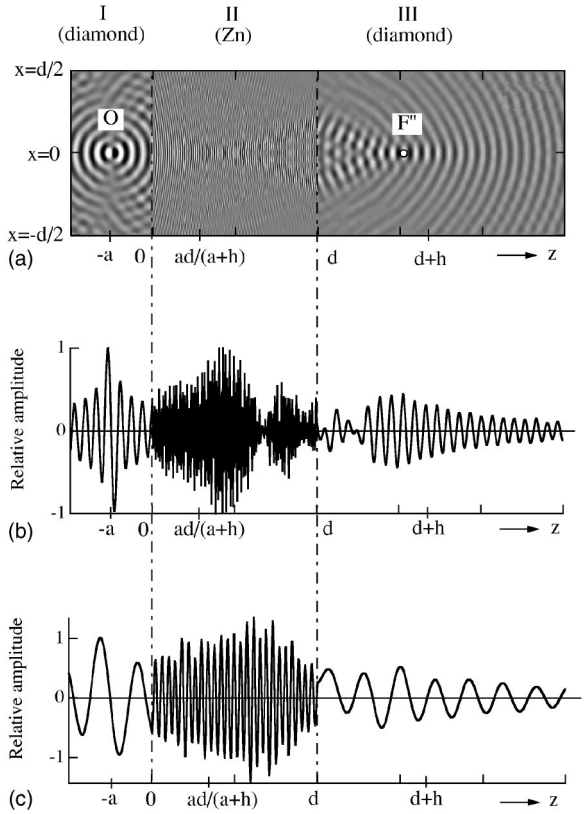

FIG. 7. (a) A snapshot of the wave amplitude in the x-z plane of the diamond-Zn-diamond system (same as for Fig. 6) calculated by a finite-difference time domain (FDTD) simulation. The excited wave in the region I is the transverse mode polarized inside the x-z plane and the polarization direction is assigned approximately parallel to the equiamplitude circular contours. The frequency assumed is $\omega=15c/d$. (b) The relative amplitude along $x=0$ of (a). (c) The relative amplitude along $x=0$ for $\omega=5c/d$. In these figures the maximum wave amplitude in region I is normalized to unity, and $a=0.25d$ and $h=0.67d$ for the comparison with Figs. 4 and 6.

phonons at a point F' ($z=1.61d$) after transmitted through the zinc slab can be seen, though not as sharp as the case with the ideal lens material [Fig. 6(b)]. This focal point F' is not identical to the point F ($z=d+h=1.67d$)) of the ideal case. However, the position of F' becomes closer to F when the angle of incidence (measured from the z axis) is restricted to a small value. The reason of this deviation of the focal point is the existence of the defocusing components that are originated from the phonons with wave vectors deflected outside the concave region of the slowness surface of a zinc slab. However, the contribution of these defocused components relative to the focused phonons is not very large.

Also the existence of sharp ridges in phonon density distribution is seen in Fig. 6(a), though they are absent for the system with an ideal lens [Fig. 4(a)]. These ridges arise from the folded structures in the group velocity curve and define the phonon caustics. Here we note again that neither the effect of transmission probability nor the effect of mode conversion at the interfaces are taken into account in these calculations.

IV. FINITE-DIFFERENCE-TIME DOMAIN (FDTD) SIMULATIONS

In the preceding sections the lensing action of an anisotropic elastic slab has been studied in the geometrical acoustic approximation and we have neglected the effects due to wave nature of phonons, such as, the diffraction and interference characteristic of finite wavelength, mode conversions, and finite transmissions and reflections at interfaces. In order to see these effects we have also performed FDTD simulations for the sound wave propagation in the same diamond-Zn-diamond system studied above. In the FDTD scheme we have solved the elastic wave equations with acoustic mismatch boundary conditions.[19] Also Mur's first-order absorbing boundary conditions[16] are applied to the outer boundaries of the assumed system. The sound waves excited at a point source (in the isotropic diamond region I) are the transverse (T) mode, which are coupled to the longitudinal (L) waves at the interfaces.

Figure 7(a) depicts the snapshot of the calculated displacement amplitude, where initial transverse waves (with the direction of polarization vector approximately parallel to equiamplitude circular contours inside the x-z plane) are excited continuously at the point O with a frequency $\omega=15c/d$ (the corresponding wavelength is $d/15$). At the interfaces between diamond and zinc both intramode (T to ST and vice versa) and intermode (T to L and vice versa) transmissions and reflections occur. These effects induced by rather large acoustic impedance mismatch between zinc and diamond as well as the deviation of the ST slowness surface in zinc from the one in an ideal material should act to destruct the focusing of phonons and sound waves in the system considered here. In spite of the presence of those effects,

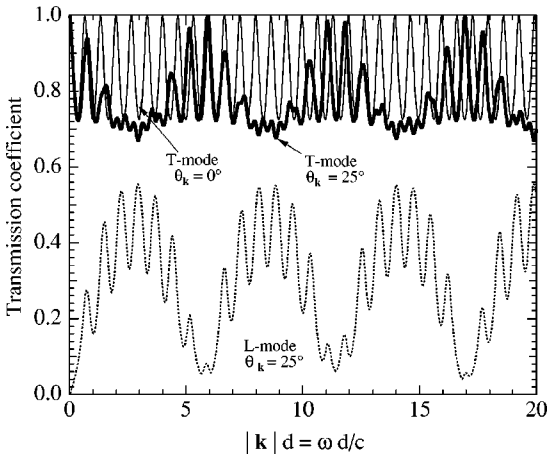

FIG. 8. The transmission coefficients of the transverse (solid lines) and longitudinal (dotted line) phonons from diamond to diamond through the zinc layer of thickness d. The horizontal axis is the normalized wave number (or frequency) in diamond. The incident wave is the transverse mode same as for Fig. 7 and the angles of incidence $\theta_{\mathbf{k}}$ in diamond measured from the z direction (the interface normal) are assumed to be 0° (thin solid line) and 25° (bold solid line and dotted line). At $\theta_{\mathbf{k}}=25°$ for the transverse mode in diamond the angle of transmission of the longitudinal mode in diamond is 37.5°. (Incidentally, the group-velocity directions in zinc is 29.7° and −17.2° for the longitudinal and transverse modes, respectively.) It should be noted that the transmission coefficient of the longitudinal phonons is zero for $\theta_{\mathbf{k}}=0°$.

however, we find that the transmitted acoustic field is focused at the point F'' near the focal point F' (about one wavelength closer to the lens) found in the ray picture [Fig. 6(a)]. We can expect that F'' becomes closer to F' as the frequency is increased further.

For comparison, the profiles of the wave amplitudes along the z axis at $\omega=15c/d$ and $\omega=5c/d$ are shown in Figs. 7(b) and 7(c), respectively. The focusing effect is more efficient at higher frequencies. Figures 7(b) and 7(c) also indicate that the transmitted amplitudes are quite large in region III, contrary to our naive expectation. Also the mode conversions due to the coupling of waves with different polarizations at layer interfaces do not seem to smear out the lensing effect. The reasons can be discussed with the help of the transmission coefficients (Fig. 8) in the diamond-Zn-diamond system described in the Appendix. First of all, we note that one of the transverse modes polarized perpendicular to the x-z plane is not excited by the initial T mode wave polarized in the x-z plane. L phonons are produced by the mode conversions at the interfaces but the resulting transmission coefficients are small at angles close to the direction normal to the layer interfaces where the focusing effect is strong for the T mode. (For the normal incidence, or $\theta_{\mathbf{k}}=0^{\circ}$ of the T waves, the mode-conversion rate to the L waves is exactly zero.) In Fig. 8 a typical example of the transmission coefficient of the L waves mode converted from the incident T waves has been shown for $\theta_{\mathbf{k}}=25^{\circ}$, the angle of T waves in diamond (region I). It becomes as large as $\simeq 0.5$ for certain ranges of frequency. For the T wave incidence the L waves in the focal region (region III) are produced by the following two processes. (A) L to L transmission at the II-III interface after the mode-converted transmission from T to L at the I-II interface. (B) ST to L conversion at the II-III interface after the T to ST mode-converted transmission at the I-II interface. In these two processes (and for $\theta_{\mathbf{k}}=25^{\circ}$) the propagation directions of the transmitted L waves in the focal region are the same and 37.5° rotated away from the normal of the interfaces. This angle is large and thus the effect of L waves produced by the mode conversion becomes important only at large propagation angles in the focal region (region III) and is small at small angles close to the normal axis where the focusing effect of the T waves is explicitly seen.

V. DISCUSSIONS AND CONCLUSIONS

Stimulated by the negative refraction of EM waves and the related topic on the photon superlens, we have considered the conditions for a bulk elastic material which works as a flat lens for phonons. Advantages of a single crystalline solid (if it works) over other possible candidates for phonon lenses such as phononic crystals is the fact that no frequency dispersion exists up to several hundred GHz and also the focusing of phonons in a three-dimensional space is possible by using hexagonal crystals with transverse isotropy. However, we have found that the shape of phonon slowness surface required for an ideal lens material should be a part of ellipsoid (concave outward) that is quite different from the one in an existing bulk crystal.

Despite this rather disappointing finding, the calculations of the transverse phonon propagation based on the ray picture shows that the majority of phonons passing through the slab of hexagonal zinc crystal with large elastic anisotropy exhibit negative refraction and are focused at a point close to the focal point of the ideal lens. This is because, for a finite range of wave vector directions around the normal of the slab lens, the shape of the slowness surface for the ST phonons in zinc coincides well with the one required for an ideal lens.

Actually, for phonons there exist three different polarizations and the associated mode conversions at interfaces of elastically dissimilar media as well as the finite-wavelength effects. The latters become significant when the wavelength is comparable to the lens thickness d, for instance. The FDTD simulations for the sound wave propagation taking account of these additional effects still reveal the focusing effect for the transmitted transverse sound waves similar to the one expected with the ray picture.

Evidently, more elaborated analysis on the lensing action of artificially designed elastic materials such as three-dimensional phononic crystals is necessary. However, our results suggest that a simple slab structure of zinc can focus phonons and sound waves emitted from a point source quite effectively. Thus, a slab of bulk solid has a potential to be used for locally concentrating vibrational energy that is radiated (in a wide range of directions) from a point source in an isotropic elastic medium. This effect can then be utilized for a heating of a small spot in an isotropic solid, for example.

The present study would stimulate to further efforts for finding or designing better anisotropic media working as a flat lens for phonons in a various frequency range. Also the

analysis and comparison with the cases of two dimensional and three dimensional phononic crystals exhibiting a lensing action should be interesting. These studies are currently under way.

ACKNOWLEDGMENTS

This work was supported in part by a Grant-in-Aid for Scientific Research from the Ministry of Education, Culture, Sports, Science and Technology (MEXT) of Japan (Grant Number 12640304), by a Grant-in-Aid for JSPS Fellows from the MEXT of Japan.

APPENDIX

In order to understand the sharpness of the focused acoustic field observed in the FDTD calculation, we analyze in this Appendix the transmission coefficients of sound waves through the diamond-Zn-diamond system. The acoustic mismatch model yields the transmission coefficients of T and L waves (incident mode is transverse) versus wave number for two typical angles of incidence $\theta_{\mathbf{k}}=0$ and $\theta_{\mathbf{k}}=25^{\circ}$ in diamond as shown in Fig. 8 (for $\theta_{\mathbf{k}}=0$ the transmission coefficient of L waves is zero). For propagation directions oblique to the layer interfaces, i.e., $\theta_{\mathbf{k}}\neq 0$, the expressions for the transmission coefficients are very complicated. But for the normal incidence $\theta_{\mathbf{k}}=0$ the two acoustic modes (T and L) comprising the sagittal mode are decoupled from each other and the transmission coefficient $|a_T|$ (defined by the modulus of the transmitted amplitude relative to the amplitude of an incident wave) of the T mode is expressed as

$$|a_T| = \left[1 + \frac{1}{4}\left(\frac{Z_{\mathrm{C}}}{Z_{\mathrm{Zn}}} - \frac{Z_{\mathrm{Zn}}}{Z_{\mathrm{C}}} \right)^2 \sin^2(\omega d/c_t) \right]^{-1/2}, \qquad \text{(A1)}$$

where Z_{C} and Z_{Zn} are the acoustic impedances of the T modes in diamond and zinc, respectively. Thus at the frequencies satisfying $\omega = n\pi c_t/d$, $(n=0,1,2,\ldots)$ the resonance occurs ($|a_T|=1$) but at $\omega=(n+1/2)\pi c_t/d$ the transmission becomes minimum and for the present case the minimum value is $|a_T|_{\min}=0.734$. Thus, we see that the transmission coefficient is rather large in spite of the fact that diamond (with $Z_{\mathrm{C}}/Z_{\mathrm{Zn}}=2.27$) is chosen for the substrate material. At an oblique angle of incidence the transmission coefficient of T waves becomes more or less smaller comparing with the case of the normal incidence but there still exist resonances for certain magnitudes of wave vectors.

[1] V. G. Veselago, Sov. Phys. Usp. **10**, 509 (1968).
[2] J. B. Pendry, Phys. Rev. Lett. **85**, 3966 (2000).
[3] M. Notomi, Phys. Rev. B **62**, 10 696 (2000).
[4] C. Luo, S. G. Johnson, J. D. Joannopoulos, and J. B. Pendry, Phys. Rev. B **65**, 201104 (2002).
[5] A. A. Houck, J. B. Brock, and I. L. Chuang, Phys. Rev. Lett. **90**, 137401 (2003).
[6] S. Foteinopoulou and C. M. Soukoulis, Phys. Rev. B **67**, 235107 (2003).
[7] P. V. Parimi, W. T. Lu, P. Vodo, J. Sokoloff, J. S. Derov, and S. Sridhar, Phys. Rev. Lett. **92**, 127401 (2004).
[8] A. Martínez, H. Míguez, A. Griol, and J. Martí, Phys. Rev. B **69**, 165119 (2004).
[9] B. C. Gupta and Z. Ye, Phys. Rev. E **67**, 036603 (2003).
[10] X. Hu, Y. Shen, X. Liu, R. Fu, and J. Zi, Phys. Rev. E **69**, 030201 (2004).
[11] J. P. Wolfe, *Imaging Phonons* (Cambridge University Press, Cambridge, 1998), Chap. 2.
[12] B. Taylor, H. J. Maris, and C. Elbaum, Phys. Rev. Lett. **23**, 416 (1969); Phys. Rev. B **3**, 1462 (1971).
[13] G. A. Northrop and J. P. Wolfe, *Nonequilibrium Phonon Dynamics* (Plenum, New York, 1985), Chap. 5.
[14] A. K. McCurdy, Phys. Rev. B **9**, 466 (1974).
[15] A. G. Every, Phys. Rev. B **34**, 2852 (1986).
[16] A. Taflove, *Advances in Computational Electrodynamics: The Finite-Difference Time-Domain Method*, edited by C. M. Soukoulis (Artech House, London, 1998).
[17] C. T. Chan, Q. L. Yu, and K. M. Ho, Phys. Rev. B **51**, 16 635 (1995).
[18] A. J. Ward and J. B. Pendry, Phys. Rev. B **58**, 7252 (1998).
[19] Y. Tanaka, Y. Tomoyasu, and S. Tamura, Phys. Rev. B **62**, 7387 (2000).
[20] Y. Tanaka, M. Takigahira, and S. Tamura, Phys. Rev. B **66**, 075409 (2002).
[21] These values $\beta=0.922$ and $\gamma=5.92$ are used for the comparison with the system consisting of a zinc slab sandwiched in between bulk diamonds to be studied in Sec. III.
[22] The second-order elastic constants we used for zinc are $c_{11}=163.7$, $c_{33}=62.93$, $c_{44}=38.68$, $c_{66}=63.71$, $c_{13}=52.48$ (in units of 10^{10} dyn cm^{-2}) that are measured by Kim *et al.*, [K. Y. Kim, W. Sachse, and A. G. Every, Phys. Rev. Lett. **70**, 3443 (1993)]. Note that $c_{12}=c_{11}-2c_{66}$ for a hexagonal crystal. The mass density is $\rho=7.14$ g cm^{-3}. These values give $R=2.09>1$, and $c_l=4.79\times10^5$ cm s^{-1} and $c_t=2.33\times10^5$ cm s^{-1} for zinc.
[23] For the transverse sound velocity of diamond we use $c=11.64\times10^5$ cm s^{-1} (mass density 3.51 g cm^{-3}). With these parameters, $\beta=0.922$, $\gamma=5.92$ and $\delta=\beta/\gamma=0.156$ for the ideal lens material to be compared with zinc.